



BIDIRECTIONAL-RESISTANT DUCTILE END DIAPHRAGMS FOR STRAIGHT STEEL BRIDGES

O. C. Celik¹ and M. Bruneau²

ABSTRACT

Ductile end diaphragms can be used both in retrofit and new design of bridges superstructures to mitigate seismic damage in other substructure and superstructure members. They have been introduced in the latest AASHTO Guide Specifications as a structural system that can be used to resist transverse earthquake effects. Here, the ductile end diaphragm concept developed for straight bridges is expanded to make it able to resist bidirectional earthquake excitations. Buckling restrained braces (BRBs) are used as the ductile fuses. Two bidirectionally-acting end diaphragm configurations (EDS-1 and EDS-2) are proposed and analytically investigated to seek the best geometrical layout to maximize the dissipated hysteretic energy. Closed form solutions are presented for practical design purposes. Strength, stiffness, and drift characteristics of the proposed configurations are quantified with an emphasis on hysteretic energy dissipation. Numerical results show that the generic bridge geometry, bidirectional loading, and the loading ratio, have a pronounced effect on the end diaphragm's inelastic behavior. In specific circumstances, each of the diaphragm concepts considered exhibit better seismic response, depending on the aspects of response that are deemed preferable in specific applications.

Introduction

End diaphragms of slab-on-girder straight steel bridges may undergo large inelastic displacements during strong earthquakes. Recent earthquake reconnaissance investigations have reported damage in bridge end diaphragms due to transverse earthquake effects (Bruneau et al. 1996, Itani et al. 2004). To reduce the seismic demands in steel bridges, several retrofitting systems have been proposed. One approach (Zahrai and Bruneau 1999; Carden et al. 2006) suggests that special ductile end diaphragms could provide an appropriate retrofit solution. This concept requires replacing existing end diaphragms with specially detailed diaphragms that can act as “seismic fuses,” i.e., which could yield prior to other substructure and superstructure elements. This concept has been experimentally verified using specially designed ductile end

¹Assoc. Prof., Div. of Theory of Structures, Faculty of Architecture, Istanbul Technical University, Taskisla, Taksim, 34437, Istanbul, Turkey

²Professor, Dept. of Civil, Structural & Environmental Engineering, University at Buffalo, Amherst, NY 14260, USA

diaphragms that have one of the following: shear panel systems (SPS), steel triangular plate added damping and stiffness devices (TADAS), eccentrically braced end diaphragms (EBF), or buckling restrained braces (BRBs). Ductile end diaphragms have been introduced in the latest AASHTO Guide Specifications (2009) as a structural system that can be used to resist transverse earthquake effects. However, in all cases considered to date, the ductile end diaphragm concepts were limited to the retrofit of bridges against earthquake excitation in the transverse direction, and had to be combined with another retrofit solution to achieve resistance in the longitudinal direction. This paper investigates the possibility of extending the ductile end diaphragm concept using BRBs to resist bidirectional earthquake effects in straight steel bridges superstructures. Two end diaphragm configurations (EDS-1 and EDS-2) are investigated to search the best geometrical layout (to maximize the dissipated energy) of the ductile end diaphragms.

Bidirectional End Diaphragm Systems with Buckling Restrained Braces (BRBs)

Two types of bracing configurations in bridge end diaphragms are considered: *End Diaphragm System-1 (EDS-1)*: Two pairs of BRBs are installed at each end of a span, in a configuration that coincides with the transverse and longitudinal directions (Fig. 1a).

End Diaphragm System-2 (EDS-2): A single pair of BRBs is installed at each end of a span, in a configuration that does not coincide with the bridge longitudinal and transverse directions (Fig. 1b).

Note that in EDS-1, the pair of BRBs oriented in the transverse direction can be connected either to the abutment or between web stiffeners of the bridge girders. The pair of longitudinal BRBs is a “new concept” and need to be connected at the abutment, either at the bearing level or on the vertical side. The braces connecting to the abutment need to be in series with lock-up devices that allow thermal expansion under normal conditions, but engage the BRBs during earthquakes. Detailing decisions depend on the existing boundary conditions of the girders. For the deck level connection, specially designed cross beams are required to elastically resist forces from the BRB, unless connection to the existing interior cross frames or girders is developed without damaging any internal component (capacity design).

Modeling Issues

Modeling of bearings, BRBs, and system idealization is given in detail in Celik and Bruneau (2007), and summarized here. Neoprene bearings, bidirectional sliding bearings, and other bearings with negligible strength to horizontal deformations (and to some degree, even bearings damaged by an earthquake that could still slide in a stable manner) are considered in this work. This case is called the “floating span.” Floating span type bridges need to be restrained laterally by devices to limit their horizontal displacements. The BRBs serve this purpose.

Both Black et al. (2002) and Sabelli et al. (2003) suggested that bilinear approximation could be used with confidence. BRBs are therefore treated as axially yielding members with cyclic symmetric elastic-plastic behavior. This helps reduce the complexity of the derived expressions. Zahrai and Bruneau (1998) demonstrated that seismic demand concentrates at the end diaphragms.

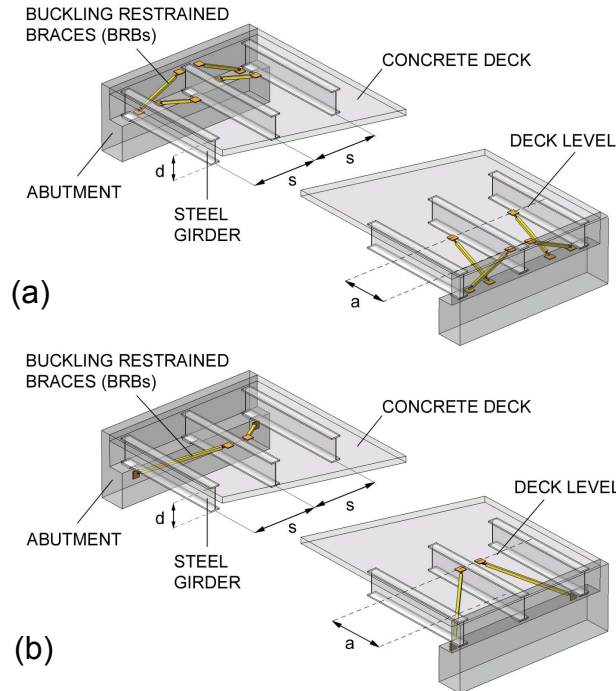


Figure 1. Bidirectional end diaphragm systems for straight steel bridges: (a) EDS-1 (b) EDS-2.

Also, the presence of intermediate cross braces does not impact the seismic behavior of slab-on-girder steel bridges and can be neglected. This leads to the development of a simplified structural model to simulate the system behavior. For EDS-1, the steps followed to idealize a typical bridge with end diaphragms into a simpler model are given in Fig. 2. A similar way is followed for EDS-2 and given in Celik and Bruneau (2007). Simplified assumptions, along with the assumed pinned end connections for BRBs, lead to a relatively simple model which is actually a three-dimensional truss supporting a rigid deck. Another assumption is that the BRBs are not active under gravity loading. Cross sectional areas of BRBs are taken to be the same for each of the two end diaphragms.

The analytical models account for general system geometric dimensions, girder spacing (s), end diaphragm depth (d) and length to internal diaphragm anchor point (a), as well as bidirectional earthquake effects. Of all of these values, the spacing of girders and the girder depth are already known if the bridge is an existing structure. The value of “ a ” could be eventually chosen to be a function of the girder spacing and would be selected based on engineering judgment (the outcome of this study could help in selecting an appropriate value for this parameter).

Behavioral Characteristics of EDS-1

Equal proportions of the total lateral load in a given direction are applied at each corner of the deck. P_L and P_T are the lateral earthquake loads acting at the deck level on one diaphragm in the longitudinal and transverse directions, respectively. Nonlinear pushover analysis is adopted in this paper. Total base shear forces in the elastic range are equal to $V_L=2P_L$ and $V_T=2P_T$, since there are two end diaphragms considered in this model.

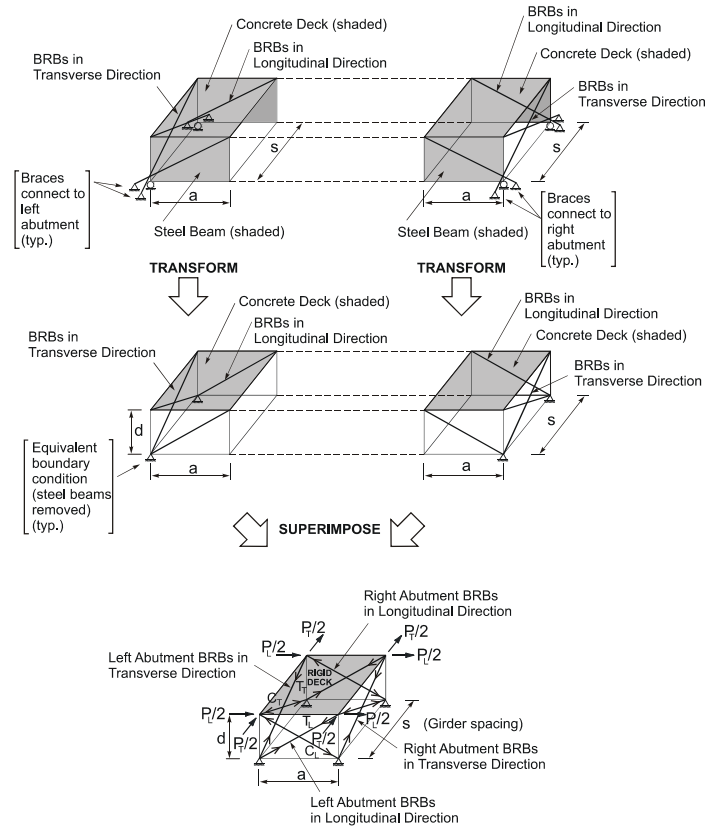


Figure 2. System idealization steps for EDS-1.

With reference to the 3D idealized truss system given in Fig. 2, BRBs axial forces ratios and their variation with bridge geometric relations are obtained for various bidirectional loading ratios and given in Celik and Bruneau (2007). P_T/P_L , C_L , T_L , C_T , T_T are the ratio of bidirectional loads, axial compression and tension forces in longitudinal and transverse BRBs, respectively. The possible limits of BRBs forces ratio and the corresponding meaning are further described below:

If $\frac{C_T}{C_L} = \frac{T_T}{T_L} > 1$, < 1 , or equals 1 then the transverse BRBs yield first, longitudinal BRBs yield first, or all BRBs yield at the same time, respectively.

In North America, it is recognized that practical numerical values for d/s fall in the range of 0.25, 0.50, 1.00, 1.25, and 1.50, covering most short and medium span slab-on-girder and deck-truss steel bridges. Also, d/a can be set equal to 0.20, 0.40, 0.60, 0.80, and 1.00 (Celik and Bruneau 2007). To account for bidirectional earthquake effects in seismic design, the 30% rule as per AASHTO (2002) and the 40% rule as per ATC-32 (1996) are selected.

Transverse BRBs Yield

Transverse Response

Fig. 3 shows a typical hysteretic curve of the end diaphragm system both in the

transverse and longitudinal directions. When $C_T, T_T > C_L, T_L$, only the transverse BRBs yield, and base shear strength (V_{yT}), yield displacement (Δ_{yT}) and corresponding drift (Δ_{yT}/d) at yield, global ductility (μ_{GT}), and the stiffness of the system (K_T) in the transverse direction are obtained depending on the bridge geometry and BRB properties as follows:

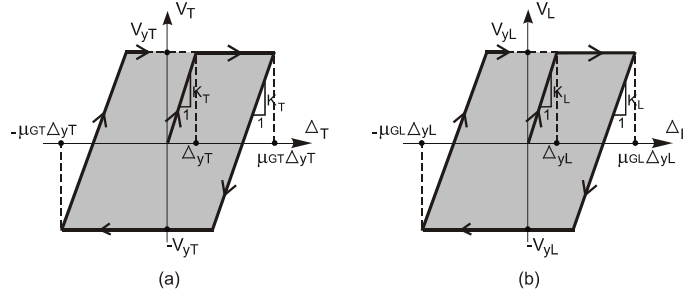


Figure 3. Base shear vs displacement hysteretic curves for end diaphragm systems: (a) Transverse direction; (b) Longitudinal direction.

$$V_{yT} = \frac{n_T}{\sqrt{1 + (d/s)^2}} (F_y A) \quad (1)$$

$$\Delta_{yT} = \frac{(s^2 + d^2)}{s} \left(\frac{F_y}{E} \right) \quad (2)$$

$$\frac{\Delta_{yT}}{d} = \frac{1 + (d/s)^2}{(d/s)} \left(\frac{F_y}{E} \right) \quad (3)$$

$$\mu_{GT} = \mu \quad (4)$$

$$K_T = \frac{n_T (d/s)}{[1 + (d/s)^2]^{3/2}} \left(\frac{EA}{d} \right) \quad (5)$$

n_T and n_L (as shown later) are the number of BRBs placed in the transverse and longitudinal directions, respectively. An equal number of BRBs in both directions are used in this study. Non-dimensional expressions have been generated to generalize these equations. For bridge design purposes, a 345MPa (50 ksi) grade unbonded steel core material with $E=200000$ MPa (29000 ksi) is assumed in this paper. Fig. 4a shows non-dimensional transverse base shear strength versus d/s curves resulting from Eq. 1. The base shear strength is observed to decrease as the d/s ratio increases, since the contribution of BRBs to the base shear strength decreases with larger direction angles measured from horizontal.

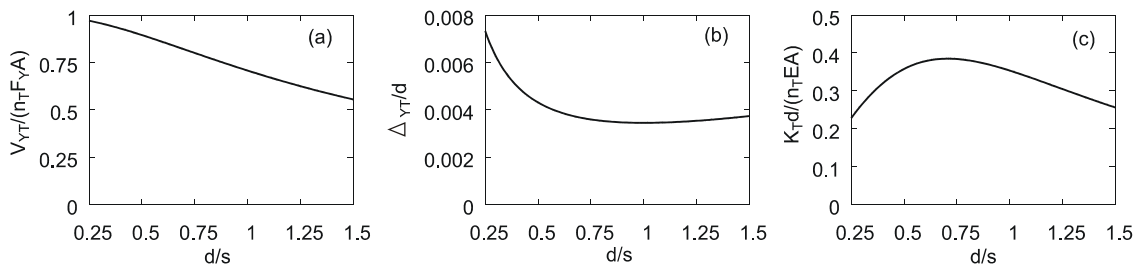


Figure 4. Transverse behavior when transverse braces yield: (a) Base shear strength vs d/s ratio; (b) Drift vs d/s ratio; (c) Stiffness vs d/s ratio.

Note that transverse drift takes its minimum value at $d/s=1$. Also, the reduction in drift is relatively smaller after $d/s=0.5$. Similarly, the variation of transverse stiffness with the d/s ratio is given in Fig. 4c. It is observed from that figure that the non-dimensional transverse stiffness is at its maximum at $d/s=0.707$. From Figs. 4b and 4c, it seems that an appropriate value for d/s should be selected between 0.5 and 1.0 if the intent is to limit transverse displacements.

Longitudinal Response

Since yielding only occurs transversely for EDS-1, BRBs in the longitudinal direction remain elastic. The longitudinal base shear, displacement, drift, and stiffness can be written as:

$$V_L = \frac{n_T(P_L/P_T)}{\sqrt{1+(d/s)^2}}(F_y A) \quad (6)$$

$$\Delta_L = \frac{s(P_L/P_T)(a^2+d^2)^{3/2}}{a^2\sqrt{s^2+d^2}}\left(\frac{F_y}{E}\right) \quad (7)$$

$$\frac{\Delta_L}{d} = \frac{(P_L/P_T)[1+(d/a)^2]^{3/2}}{(d/a)\sqrt{1+(d/s)^2}}\left(\frac{F_y}{E}\right) \quad (8)$$

$$K_L = \frac{n_T(d/a)}{[1+(d/a)^2]^{3/2}}\left(\frac{EA}{d}\right) \quad (9)$$

Non-dimensional base shear and drift are also dependent on the previously defined bidirectional load ratio (P_L/P_T or P_T/P_L). The widely accepted 30% rule is used in developing the forthcoming diagrams in this paper. Further details of these derivations and the diagrams obtained for the 40% rule can be found in Celik and Bruneau (2007). Fig. 5a shows the variation of base shear as a function of end diaphragm geometric ratios. There is a decrease in this value as the d/s ratio increases due to larger direction angles resulting in smaller horizontal force components. The variation of longitudinal drift as a function of end diaphragm geometric ratios and the P_L/P_T value are shown in Fig. 5b. For a constant d/s , these curves reveal that longitudinal drift becomes minimum at $d/a=0.707$. However, as seen on the same figure, when the ratio of d/a is greater than 0.5, the variation in drift is relatively insignificant, suggesting that appropriate d/a ratios could be selected between 0.5 and 1.0, if the intent is to minimize drift. Again, Fig. 5c shows that maximum non-dimensional longitudinal stiffness is reached at $d/a=0.707$.

Hysteretic Energy Dissipation

Generally, the total hysteretic energy dissipated in one cycle is the sum of the areas under the global hysteretic curves in both directions (i.e., summation of the areas under Figs. 3a and 3b), or simply equal to the energy dissipated by the yielding BRBs. The following expression gives the volumetric energy dissipation for the system considered:

$$\frac{E_H}{\text{Vol.}} = \frac{4(\mu-1)}{1 + \frac{(d/s)}{(d/a)} \sqrt{\frac{1+(d/a)^2}{1+(d/s)^2}}}\left(\frac{F_y^2}{E}\right) \quad (10)$$

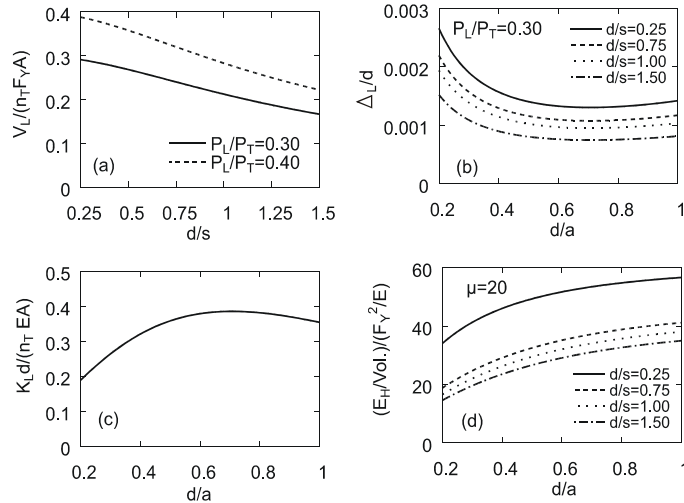


Figure 5. Longitudinal behavior when transverse BRBs yield: (a) Base shear vs d/s ratio for $P_L/P_T=0.30$ and 0.40 ; (b) Drift vs d/a ratio for $P_L/P_T=0.30$; (c) Stiffness vs d/a ratio; (d) Volumetric energy dissipation vs end diaphragm geometric ratios for $\mu=20$.

The variation of hysteretic energy dissipation per brace volume is plotted in Fig. 5d for $\mu=20$, revealing that non-dimensional dissipated hysteretic energy increases as d/a increases for constant values of d/s (which could be important in an existing bridge retrofit design), but decreases as d/s increases for constant values of d/a (which could be important in a new bridge design). However, as observed on the relevant diagrams, the decrease in energy dissipation is relatively less for larger values of d/s .

The behavior when longitudinal BRBs yield can be investigated in a similar manner. For this case, closed form solutions and developed diagrams can be found in Celik and Bruneau (2007).

Behavioral Characteristics of EDS-2

Bidirectional loading and BRBs forces for EDS-2 are shown in Fig. 6. When the value of axial forces for the BRBs in the DT direction is greater than for the braces in the DL direction, axial yielding in the DT braces occurs. The practical values of the s/a ratio are set to 0.25, 0.50, 0.75, 1.00, 1.25, and 1.50. Bidirectional response develops under bidirectional loading.

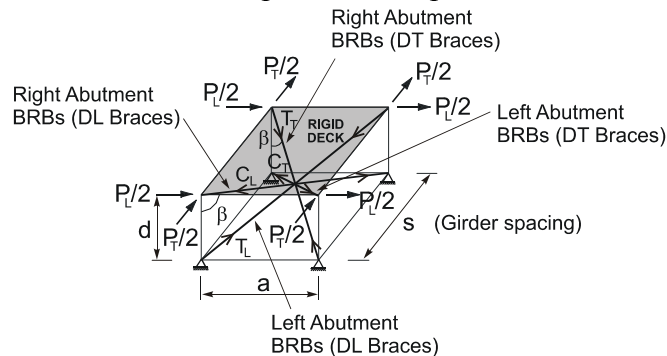


Figure 6. Bidirectional loading and BRBs forces for EDS-2.

DT BRBs Yield

Transverse Response

Using the non-dimensional properties, the transverse base shear strength, yield drift, global displacement ductility (μ_{GT}) and the stiffness can be expressed as:

$$V_{yT} = \left[\frac{4(s/a)}{\sqrt{1 + (s/a)^2 + (d/a)^2} [1 - (s/a)(P_L/P_T)]} \right] (F_y A) \quad (11)$$

$$\frac{\Delta_{yT}}{d} = \frac{[1 + (s/a)^2 + (d/a)^2]}{(s/a)(d/a)[1 - (s/a)(P_L/P_T)]} \left(\frac{F_y}{E} \right) \quad (12)$$

$$\mu_{GT} = \left[\frac{[1 - (s/a)(P_L/P_T)]\mu + [1 + (s/a)(P_L/P_T)]}{2} \right] \quad (13)$$

$$K_T = \left[\frac{4(s/a)^2 (d/a)}{[1 + (s/a)^2 + (d/a)^2]^{3/2}} \right] \left(\frac{EA}{d} \right) \quad (14)$$

These characteristics are demonstrated in Figs. 7a through 7d. When the DT braces yield, the base shear decreases as d/a increases for constant values of s/a and decreases as s/a decreases for constant values of d/a (i.e., smaller base shears are obtained at smaller β angles). Drift (Δ_{yT}/d) decreases as d/a increases, revealing that BRBs with larger direction angles would be preferable to obtain stiffer diaphragms. For a constant value of d/a , drift decreases as s/a increases, showing that EDS-2 is more effective when sufficient girder spacing exists. The change in drift is less for larger values of s/a . Global ductility (μ_{GT}) decreases as s/a increases. Expectedly, for constant values of s/a , the global ductility increases as the local (BRB) ductility (μ) increases. Stiffness increases as d/a and s/a ratios increase. However, this increase is less after values of $d/a=0.60$.

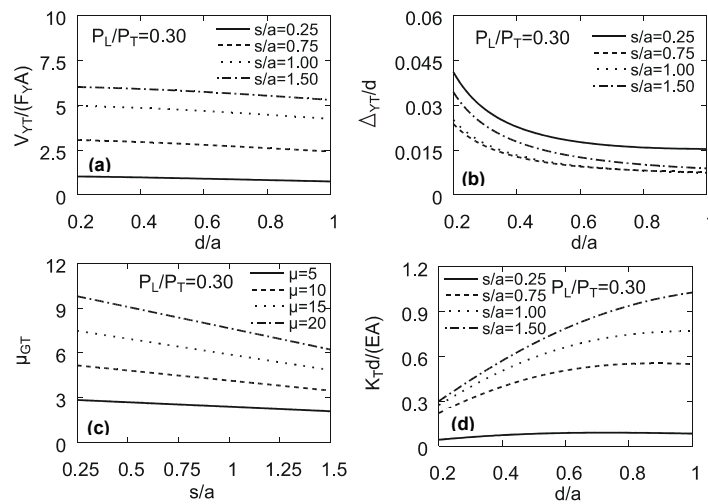


Figure 7. Transverse behavior when DT BRBs yield: (a) Base shear vs d/a ratio for $P_L/P_T=0.30$; (b) Drift vs d/a ratio for $P_L/P_T=0.30$; (c) Global ductility ratio vs s/a ratio and local ductility for $P_L/P_T=0.30$; (d) Stiffness vs d/a and s/a ratios.

Longitudinal Response

The base shear, yield drift, global ductility, and stiffness in the longitudinal direction are:

$$V_{yL} = \left[\frac{4(s/a)(P_L/P_T)}{\sqrt{1+(s/a)^2+(d/a)^2}[(s/a)(P_L/P_T)-1]} \right] (F_y A) \quad (15)$$

$$\frac{\Delta_{yL}}{d} = \frac{[1+(s/a)^2+(d/a)^2](s/a)(P_L/P_T)}{(d/a)[1-(s/a)(P_L/P_T)]} \left(\frac{F_y}{E} \right) \quad (16)$$

$$\mu_{GL} = \left[\frac{[(s/a)(P_L/P_T)-1]\mu + [(s/a)(P_L/P_T)+1]}{2(s/a)(P_L/P_T)} \right] \quad (17)$$

$$K_L = \left[\frac{-4(d/a)}{[1+(s/a)^2+(d/a)^2]^{3/2}} \right] \left(\frac{EA}{d} \right) \quad (18)$$

Variation of these behavioral characteristics is shown in Figs. 8a through 8d.

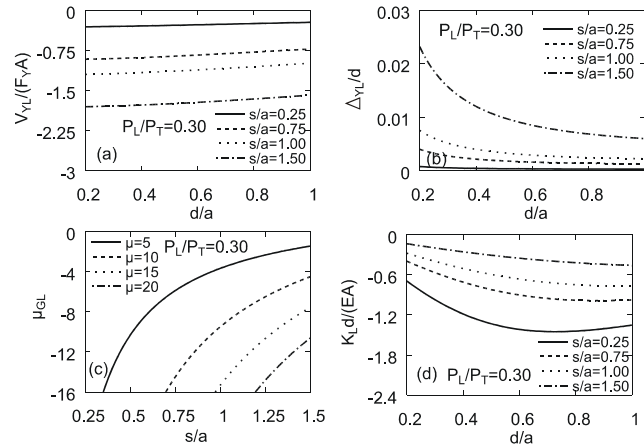


Figure 8. Longitudinal behavior when DT BRBs yield: (a) Base shear strength vs d/a ratio for $P_L/P_T=0.30$; (b) Drift vs d/a ratio for $P_L/P_T=0.30$; (c) Global longitudinal ductility ratio vs s/a ratio and local ductility for $P_L/P_T=0.30$; (d) Stiffness vs d/a and s/a ratios.

Hysteretic Energy Dissipation

Volumetric hysteretic energy dissipated through a full cycle of displacement is written as follows:

$$\frac{E_H}{Vol.} = 2(\mu - 1) \left(\frac{F_y^2}{E} \right) \quad (19)$$

The behavior when DL BRBs yield can be investigated in a similar manner. For this case, closed form solutions and developed diagrams can be found in Celik and Bruneau (2007).

Conclusions

Some shortcomings of the known ductile end diaphragm concepts have been resolved using the selected bidirectional ductile bracing configurations with BRBs. Analytical investigations suggest that an appropriate value for d/s for optimal seismic response could be between 0.5 and 1.0. When the ratio of d/a is greater than 0.5, the variation in longitudinal drift is relatively insignificant, suggesting that appropriate d/a ratios could also be selected between 0.5 and 1.0. For constant values of s/a , the global ductility increases as the local (BRB) ductility (μ) increases. The proposed end diaphragm systems are promising and viable compared to the alternatives commonly used in bridge seismic retrofit or new design applications.

Acknowledgments

This research was supported by the Federal Highway Administration (FHWA).

References

- American Association of State Highway and Transportation Officials (AASHTO), 2002. *Standard Specifications for Highway Bridges*, Washington, D.C.
- American Association of State Highway and Transportation Officials (AASHTO), 2009. *Guide Specifications for LRFD Seismic Bridge Design*, Washington, D.C.
- Applied Technology Council (ATC-32), 1996. *Improved Seismic Design Criteria for California Bridges: Provisional Recommendations*, California-Washington, D.C.
- Black, C., N. Makris, and I. Aiken, 2002. Component testing, stability analysis and characterization of buckling-restrained unbonded braces, *PEER Report 2002/08*, University of California, Berkeley.
- Bruneau, M., J.C. Wilson, and R. Tremblay, 1996. Performance of steel bridges during the 1995 Hyogo-ken Nanbu (Kobe, Japan) earthquake, *Can J Civ Eng* 23, 678-713.
- Carden, L.P., A.M. Itani, and I.G. Buckle, 2006. Seismic performance of steel girder bridges with ductile cross frames using buckling-restrained braces, *J Struct Eng ASCE* 132 (3), 338-345.
- Celik, O.C., and M. Bruneau, 2007. Seismic behavior of bidirectional-resistant ductile end diaphragms with unbonded braces in straight or skewed steel bridges, *Technical Report MCEER-07-0003*, MCEER-Earthquake Engineering to Extreme Events, Buffalo, NY.
- Itani, A.M., M. Bruneau, L. Carden, and I.G. Buckle, 2004. Seismic behavior of steel girder bridge superstructures, *J Bridge Eng ASCE-Special Edition on Steel Bridges* 9 (3), 243-249.
- Sabelli, R., S. Mahin, and C. Chang, 2003. Seismic demands on steel braced frame buildings with buckling-restrained braces, *Eng Struct* 25 (5), 655-666.
- Zahrai, S.M., and M. Bruneau, 1998. Impact of diaphragms on seismic response of straight slab-on-girder steel bridges, *J Struct Eng ASCE* 124 (8), 938-947.
- Zahrai, S.M., and M. Bruneau, 1999. Ductile end-diaphragms for seismic retrofit of slab-on-girder steel bridges, *J Struct Eng ASCE* 125 (1), 71-80.